Change Detection of Lacustrine Soils in Abis Region, Alexandria Governorate, Egypt

Hoda A. Mahmoud[1], I. Morsy[2], Ola S. Elwany[1], I.I, Abou Elseoud[1]

[1] Department of Soil and Agricultural Chemistry, Faculty of Agriculture, Saba Basha, Alexandria University, Egypt.

[2] Soil, Water and Environment Res. Inst. (SWERI), Agricultural Research Center (ARC), Giza, Egypt

DOI: 10.21608/ajsws.2025.416469.1025

Article Information

Received:August 21th 2025

Revised:September 14 2025

Accepted: September 25st 2025

Published:October 21st 2025

ABSTRACT: This study aims to investigate and document the changes that have occurred in the land over time, with a particular emphasis on analyzing the physical and chemical properties of the soil to compare its condition between the years 2005 and 2024. The study area, 109.6 Feddan, is situated in Village 10, Abis region, specifically within the governorate of Alexandria, Egypt. This study used several datasets, specifically Landsat satellite imagery for 2024. A total of 48 soil samples were taken (24 surface and 24 subsurface), covering a total area of 88.7 Feddan. physical and chemical properties of soil and water samples, such as texture, EC, pH, soluble cations and anions, (SAR), calcium carbonate $CaCO_3$, organic matter content, available nitrogen, phosphorus, and potassium, were measured. To create the digital maps of the study area for 2024, it was necessary to enter spatial data (points, lines, areas) and link them to metadata (numbers, text). The results revealed a noticeable increase in the soil content of calcium carbonate in 2024 compared to 2005, along with a rise in soil salinity, organic matter content, and the available phosphorus and potassium levels. Conversely, there was a reduction in soil depth and available nitrogen content. Regarding soil texture, a complete transformation was observed; in 2005, the texture was classified as *clay* and *clay loam*, whereas in 2024, it shifted to *loam*, *sandy clay loam*, and *sandy loam*. The results of this comparison contribute to improving land management strategies and guiding agricultural policies in a scientifically sound manner.

Keywords: Lacustrine soils, Abis region, Change detection, GIS .

INTRODUCTION: Lacustrine soils are a fundamental and enduring part of natural ecosystems, with which both environmental stability and human activities are closely linked. These soils form through the gradual deposition of sediments at the bottom of ancient lakes and play a key role in maintaining ecological balance **(Agatova et al., 2023, and Perego et al., 2025).** Nevertheless, these sensitive lake and wetland environments are increasingly threatened by human influence and climate change. Soil properties in such areas often shift due to changes in water dynamics, plant communities, and land use patterns **(Sun et al., 2018, Rudaya et al., 2021,and Wang et al., 2022).** The drying of lake beds has given rise to unexpected issues, particularly impacting agricultural productivity and local economies **(Montero-Rosado et al., 2023).** As a result, monitoring and analyzing changes in the characteristics of lacustrine soils is essential for assessing environmental consequences and shaping sustainable land management practices **(Yang et al., 2021, Stringer and Prendergast,2023, and Zheng et al., 2024).**

The notion of change detection has undergone considerable evolution over time, influenced by technological advancements and the heightened significance of this methodology across diverse fields **(Hemati et al., 2021).** Accurate and reliable change detection in land cover and land use is essential for comprehending the interplay between human actions and natural processes. This understanding is imperative for making informed decisions, as it enables the monitoring of landscape alterations over time and evaluates their effects on sustainable development **(Yossif, 2017).** Both temperature and moisture levels are essential in controlling the speed of key soil formation processes **(Vetráková, 2023).** Soil development is also strongly influenced by elevation and nutrient availability **(Wu et al., 2021).** Many researches demonstrated the impact of organic substance oxidation on soil properties, leading to changes in soil characteristics **(Parker and Prabawa, 2020).** Additionally, changes in soil structure, especially when soil horizons fail to develop due to altered climatic conditions, are difficult to detect without long-term monitoring programs **(Bungau et al., 2021).**

Change detection serves to extract valuable insights that facilitate enhanced decision-making **(Liu et al., 2024).** This procedure entails the visual identification of differences in images captured from the same location at different intervals **(Onishi and Ise, 2021).** Variations in soil texture may arise from factors such as drought, rainfall, vegetation growth, or anthropogenic activities, including vehicle or pedestrian movement **(Jim, 2023).**

Historically, the concept of change detection is rooted in the early developments of image processing and computer vision, where researchers sought to identify alterations in visual data over time **(Wen et al., 2021).** The utilization of bi-temporal images, which are defined as pairs of images captured at different temporal intervals, laid the groundwork for systematic approaches in change detection **(Jiang et al., 2024).** This fundamental methodology has progressed to encompass more advanced techniques that address the challenges presented by various environmental factors, which often impede the detection of meaningful changes **(Kuehne et al., 2025).**

The change detection methods under evaluation comprise image differencing, vegetation index differencing, selective principal components analysis (SPCA), direct multi-date unsupervised classification, post-classification change differencing, and a synergy of image enhancement with post-classification comparison **(Mas, 1999).** These methods are typically divided into content-driven and layout-driven approaches **(Prazina et al., 2023).** Content-driven methods focus on the intelligent extraction and analysis of image elements to identify discrepancies, whilst layout-driven methods utilize structural characteristics to detect changes in document formats **(Banian, 2021).** The study of change detection employing multi-temporal images has been extensively conducted, involving the acquisition of two image pairs at separate intervals. One pair consists of a reference image captured during the earlier period and a test image from the subsequent period. This test image is examined in conjunction with the reference image to predict the changes **(Almutairi and Warner, 2010, and Du et al., 2013).** The second set of images includes a reverse reference image and a reverse testing image, wherein the prediction is inverted, and changes are anticipated from the reference band to the earlier testing band. To address this, a novel method for change detection has been proposed **(Fisichella and Garolla, 2021,and Ma et al., 2024).** In recent years, the scope of applications for change detection has significantly expanded **(Shi et al., 2020).**

2. Materials and Methods

2.1. The study area

2.1.1. Location

The study area, 109.6 Feddan (45.86 hectares) is situated in Village 10, Abis region, specifically within the governorate of Alexandria, Egypt. It is located to the south of Alexandria city. The study site is positioned around coordinates 31°9'30" to 31°10'10" N latitude and 29°57'50" to 29°58'40" E longitude (Map 1), encompassing a "North area 66.03 Feddan (27.63 hectares)" and "East area 22.7 Feddan (9.5 hectares)" and a central "fish farm 20.8 Feddan (8.7 hectares)".

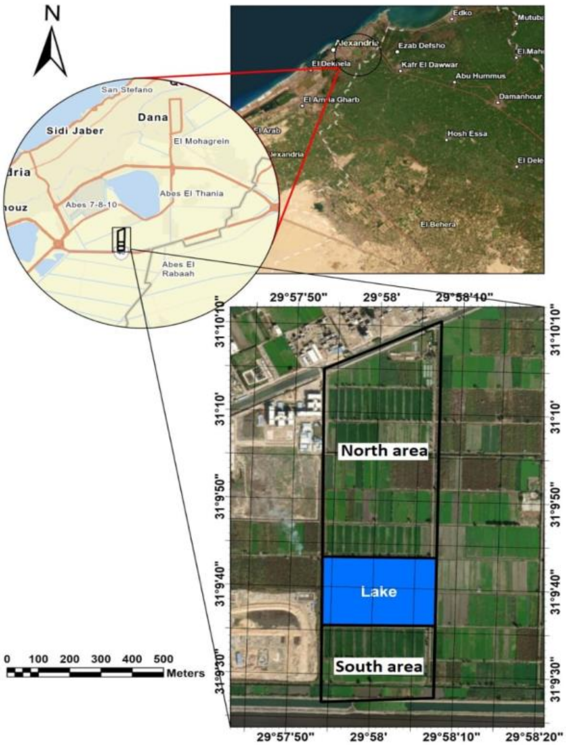

Map 1: General location of the study area

2.1.2. Climate

The climate of the Northern Delta is typically Mediterranean. Because of the proximity to the Mediterranean and Lake Maryout. The warmest months are July and August, with average maximum temperatures of around 30°C, while January is the coolest month, with an average minimum of 9.1°C. Rainfall is highest in January (52 mm) and nearly absent from June to August, indicating a dry summer period. Humidity levels remain relatively stable throughout the year, peaking slightly in December. Wind speeds are moderate, with May experiencing the highest average at 18 km/h. Sunshine hours are greatest in the summer, particularly July, which sees up to 330 hours of sunlight. Meteorological data were taken from the NASA Prediction of Worldwide Energy Resource (POWER)- Climatology Resource for Agroclimatology website (http://power.larc.nasa.gov/), tabulated, and evaluated to derive monthly averages.

2.1.3. Geology and Geomorphology

The geological deposits in the area belong to the Holocene age **(Said, 1990).** The soil of the study area was derived from the Lacustrine deposits of Maryout Lake, with an elevation of about 2.5 m below sea level with an almost flat surface. These deposits are characterized by stratified and salt effects. Shells are commonly in an irregular distribution.

2.1.4. Irrigation and Drainage Systems

The main irrigation system is surface, with water from El Mahmodia canal. The drainage system in the studied area is tile drains, with moderate efficiency **(Yehia et al,.2014).** Due to heavy losses from the existing irrigated area, the water table has already risen to within 150 cm of the surface in some parts of the new lands, resulting in waterlogging and secondary salinization. Drainage network is now urgently needed in these areas **(IFAD, 1991).**

2.2. Data sets and Soil Survey

This study used several datasets, specifically Landsat satellite imagery for 2024, as well as maps derived from satellite images captured in 2005. A total of 48 soil sample observations were taken (24 surface and 24 subsurface), covering a total area of 88.7 Feddan. These drill observations were identified using GPS, and On-site drill observations were described according to soil morphological variations, such as soil color, slope, and depth, as reported by **Stuart-Street et al. (2020).** These observations were obtained from the U.S. Geological Survey's Earth Explorer program (USGS) (https://earthexplorer.usgs.gov).

A soil survey was carried out in the area through digging soil pits and auger observations. And soil samples were collected for laboratory determinations. (Map 2) shows the location of the soil observations, and the layout of parcels in the study site. Water samples collected: (1) irrigation water samples and (1) drainage water. Samples were collected from the main irrigation and drainage channels for the study area.

2.3. Laboratory Analysis The soil samples were air dried, passed through a 2mm sieve, and then stored for analysis **(Jackson, 1973).** The following determinations were carried out:

2.3.1. Soil Physical Analysis

Soil texture was determined according to Page et al (1982).

2.3.2. Soil and Water Chemical Analysis

Soil chemical characteristics were measured according to Page et al (1982), which included soil reaction (pH), electric conductivity (EC dS/m), soluble cations and anions, and sodium adsorption ratio (SAR), and total calcium carbonate percent, which were determined by calcimeter. Also, water samples (irrigation and drainage) were analyzed for cations and anions according to Page et al (1982).

2.3.3.Soil Nutritional Analysis

Soil nutritional properties determinations included organic matter content according to Walkley and Black rapid titration method **(Jackson, 1973)**, available nitrogen, available phosphorus, and available potassium were determined by Richards (1954).

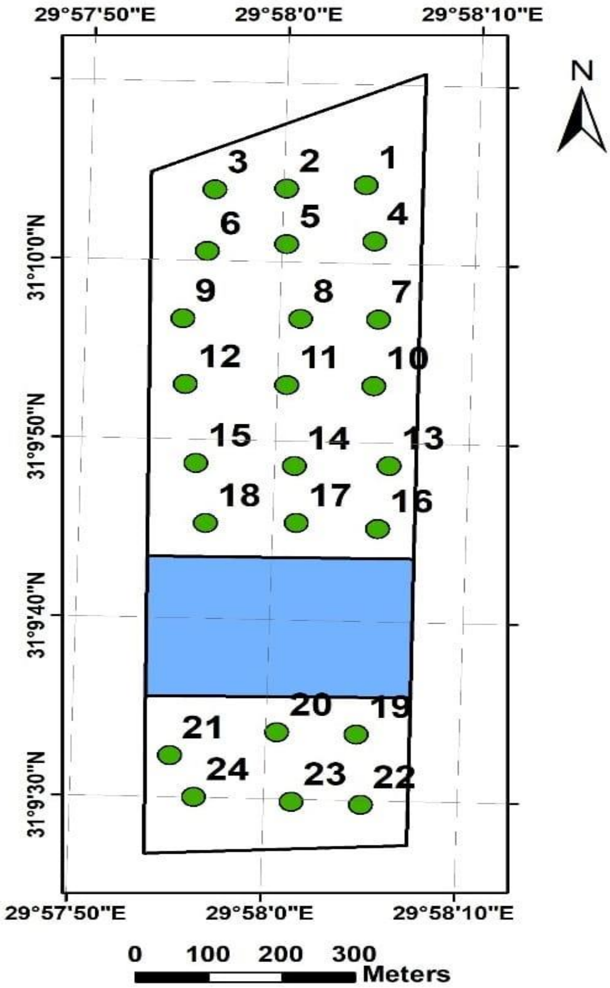

Map (2). Location of soil observations in the study area.

2.4. GIS Maps of soil properties:

The attribute data includes data for several physical and chemical soil properties, both field and laboratory-based. To create the digital maps of the study area for 2024, it was necessary to enter spatial data (points, lines, areas) and link them to metadata (numbers, text). These data were obtained from field and laboratory measurements using ArcGIS Pro 2.7, a mapping software that supports both raster and vector data (ESRI, 2021). The data entry processes were reviewed and corrected through a series of steps, resulting in several maps of some soil properties. Previous data for the study area for 2005, obtained in the same year, were also reprocessed and prepared for comparison and detection of changes between them.

3. Results and Discussion

Soil Characterization

Some physical, chemical, and nutritional soil characterization:

The results of the data examination from the laboratory and statistical analyses are shown in Table (1). Based on the results of field observation analyses, maps of some soil properties were prepared. On the other hand, the chemical properties of irrigation and drainage water are presented in table(2).

Table (1). Statistical parameters of soil properties

soil property	Maximum	Minimum	Mean	Standard Deviation	Variance	CV%
pH	8.5	8	8.31	0.12	0.01	1.44
pH sub	8.7	8	8.42	0.2	0.04	2.38
T.Carbonate%	22.1	16.9	19.23	1.39	1.92	7.23
T.C sub%	27.6	17.2	21.14	3.01	9.04	14.24
EC(ds/m)	3.7	0.6	1.58	0.89	0.79	56.33
EC sub(ds/m)	5.4	0.4	1.61	1.02	1.04	63.35
SAR	3.36	0.38	1.51	0.89	0.8	58.94
SAR sub	4.24	0.23	1.67	1.18	1.4	70.66
O.M%	2.2	1.3	1.85	0.22	0.05	11.89
K(mg/kg)	145	40	89.54	25.97	674.69	29.00
P(mg/kg)	23.1	14.2	17.58	2.48	6.16	14.11
N(mg/kg)	8.3	2.2	3.28	1.26	1.59	38.41

Table(2). Some physical and chemical irrigation and drainage water characterization Change detection in the study area during the periods 2005 and 2024:

No	pH	EC (ds/m)	Na (meq/l)	Cl (meq/l)	Ca (meq/l)	Mg (meq/l)	K (meq/l)	HCO_3^- (meq/l)	SO_4^- (meq/l)	SAR
Irrigation	7.8	1.7	2	10.9	8	4	2.5	1.2	4.1	0.82
Drainage	7.9	2	3.9	12.9	8	5	2.9	1.6	4.9	1.53

Studying changes in land characteristics is a fundamental tool for understanding the development of local environments and the impact of both natural factors and human activities over time. The area under investigation holds particular importance due to its agricultural uses, geographical location, and its exposure to various climatic and administrative influences over the past decades.

This study aims to assess the changes that have occurred in the soil properties of the study area between the years 2005 and 2024. A scientifically sound comparison was carried out, maintaining the same measurement methodology in both periods to ensure objective and accurate results. The studied properties include calcium carbonate content, soil depth, salinity level, soil texture, organic matter content, and available N, P, K, among other key characteristics that serve as indicators of soil health and productivity.

The results of the study are presented through maps (from Map3 to Map10) and comparative tables that highlight both quantitative and qualitative differences between the two years (from Table 3 to Table 10). These findings contribute to a better understanding of environmental trends and support future agricultural and environmental planning in the area.

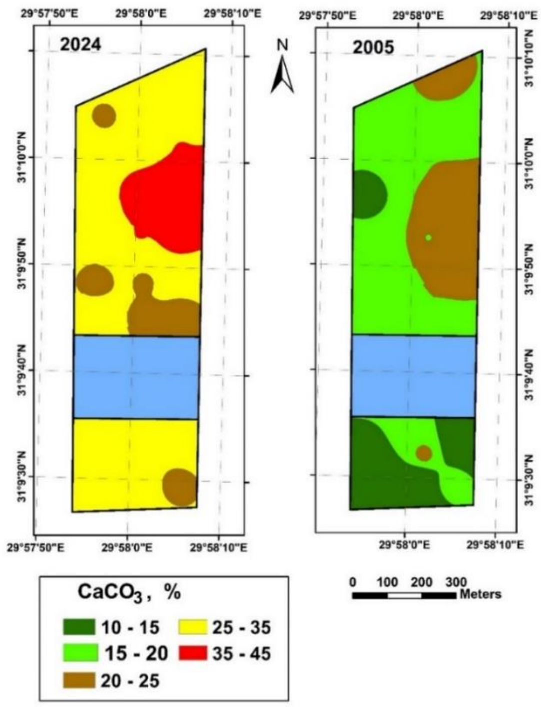

Map (3) Distribution of CaCO3 and changes detected between 2005 and 2024 in the study area

Table (3) Areas and percentages of CaCO3 classes

2024				2005			
CaCO3%	Hectares	Feddan	%	CaCO3 %	Hectares	Feddan	%
20-25	4.67	11.15	12.57	10-15	7.57	18.09	20.39
35-25	26.72	63.87	71.97	15-20	20.54	49.08	55.31
45-35	5.74	13.72	15.46	20-25	9.03	21.57	24.31
Total	37.13	88.74	100		37.13	88.75	100

Assessment of the calcium carbonate map, spatial analysis indicates a significant rise in CaCO3 concentration between 2005 and 2024. While 55% of the study area fell within the 15-20% CaCO3 range in 2005, by 2024 this shifted markedly toward higher concentrations, with 72% of the area registering 25-35% CaCO3. Agricultural conversion of desiccated lacustrine systems drives authigenic CaCO3 enrichment through anthropogenic amplification of natural hydrogeochemical processes: 1) irrigation with bicarbonate-rich waters (e.g., $[Ca^{2+}] > 200$ mg/L) induces evaporative precipitation of pedogenic calcite (Minhas et al., 2024), while 2) organic fertilizer mineralization generates low-molecular-weight organic acids (e.g., oxalic, acetic) that transiently dissolve primary carbonates, liberating Ca^{2+} for reprecipitation as secondary calcretes in alkaline microsites (Li et al., 2023), 3) synthetic fertilizers ($NH_4NO_3 \rightarrow HNO3$) and tillage further amplify this dissolution-reprecipitation cycle (Zamanian et al., 2021; Duniway et al., 2010), collectively elevating surficial $CaCO_3$ inventories by 20–45% and enhancing accumulation rates by ≤300% versus pre-agricultural baselines (Cohen, 2023).

Table (4) Areas and percentages of Depth classes

Description	Depth	2024			2005		
	(cm)	Hectares	Feddan	%	Hectares	Feddan	%
Sallow	50-60	23.20	55.46	62.49			
Moderately deep	60-75	13.93	33.28	37.51	29.57	70.66	79.62
	75-90				7.57	18.08	20.38
	Total		88.74	100	37.13	88.75	100

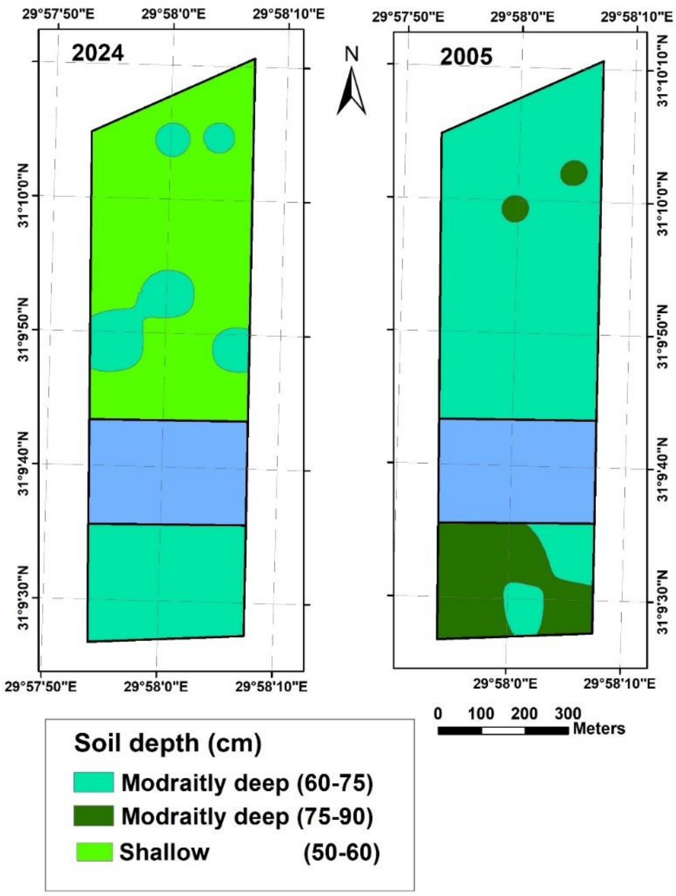

Map (4) Distribution of Soil depth and changes detected between 2005 and 2024 in the study area

Assessment of the soil depth map suggests an increase in the groundwater level in 2024 as compared to 2005. The analysis further shows that in 2024, approximately 62.5% of the land area had a soil depth of 50-60 cm. On the other hand, in 2005, 79.6% of the area had a soil depth of 60-75 cm, indicating a significant increase in groundwater level in 2024 as compared to 2005. The increase in groundwater level is as a result of the prolonged cultivation of paddy rice on clay soils with long-term inadequate drainage systems. The inundation of the fields during the rice-growing season led to the formation of a perched groundwater table, which reduced the ability of water to move through the soil as a result of puddling-induced destruction of macropores (Bouman et al., 2007). The post-harvest period saw significant groundwater flow obstruction as a result of the clay soil's low porosity and severely blocked drainage systems (Dingman, 2015), which led to stagnant groundwater and water table recession during cultivation cycles, thus allowing progressive groundwater rise (Ritzema, 1994; Kirk, 2004).

Table(5) Areas and percentages of Salinity classes

Soil salinity		2024			2005		
Description	dS/m	Hectare	Feddan	%	Hectare	Feddan	%
Non saline	< 2	2.94	7.02	7.91	7.85	18.77	21.15
Moderately saline	2-3	18.08	43.21	48.69	10.91	26.07	29.39
	3-4	8.93	21.34	24.04	5.02	11.99	13.51
Saline	4-5	4.85	11.59	13.06	9.73	23.26	1.16
	5-6	1.65	3.95	4.45	3.27	7.81	8.80
	6-7	0.69	1.64	1.85	0.35	0.84	0.94
	Total	**37.13**	**88.75**	**100.00**	**37.13**	**88.73**	**100**

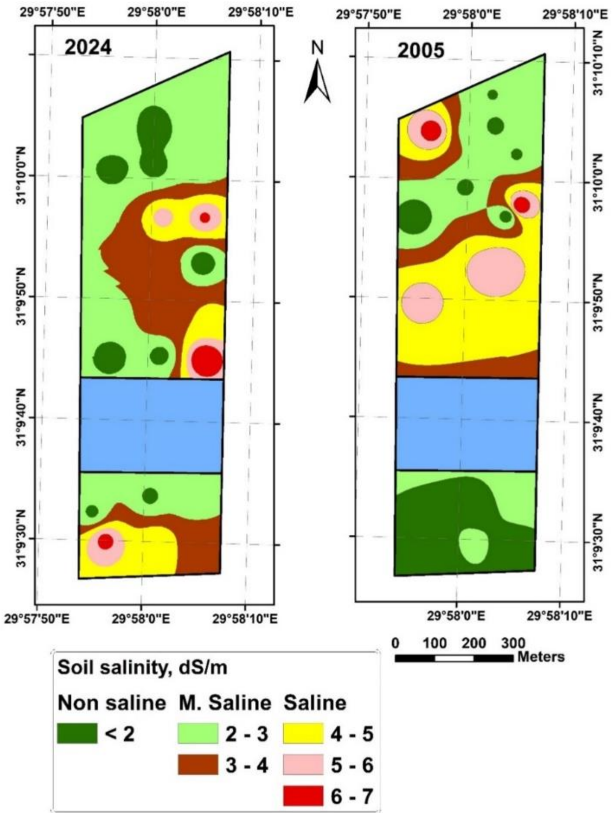

Map(5) Distribution of Salinity and changes detected between 2005 and 2024 in the study area

Salinity mapping reveals a pronounced increase in soil salinity across the study area in the current survey compared to 2005. Over 19% of the land area now exceeds 4 dS m^{-1} electrical conductivity (EC), marking a near-doubling of saline extent relative to 2005, when only ~10% of the area surpassed this threshold – effectively classifying these zones as saline soils according to contemporary standards (FAO, 2021). In this semi-arid zone, hyper-evaporative conditions (Walter et al., 2023) synergize with shallow groundwater (<1.0 m) to drive capillary solute flux, while $CaCO_3$ enrichment (>5%) elevates pH (>8.5), triggering calcite precipitation and Ca^{2+} depletion that exacerbates sodicity (Minhas et al., 2024). Concurrently, legacy rice-puddling creates a subsoil permeability barrier (Zhang et al., 2023), suppressing leaching. This pedo-climatic triad concentrates salts via terminal evaporative sequestration.

Table(6) Areas and percentages of Texture classes

	2024			2005		
Texture	**Hectares**	**Feddan**	**%**	**Hectares**	**Feddan**	**%**
Clay				23.60	56.41	63.57
Clay loam	5.51	13.17	14.84	13.53	32.33	36.43
loam	13.57	32.43	36.54			
Sandy clay loam	14.86	35.52	40.12			
sandy loam	3.19	7.63	8.60			
total	**37.13**	**88.74**	**100**	**37.13**	**88.74**	**100**

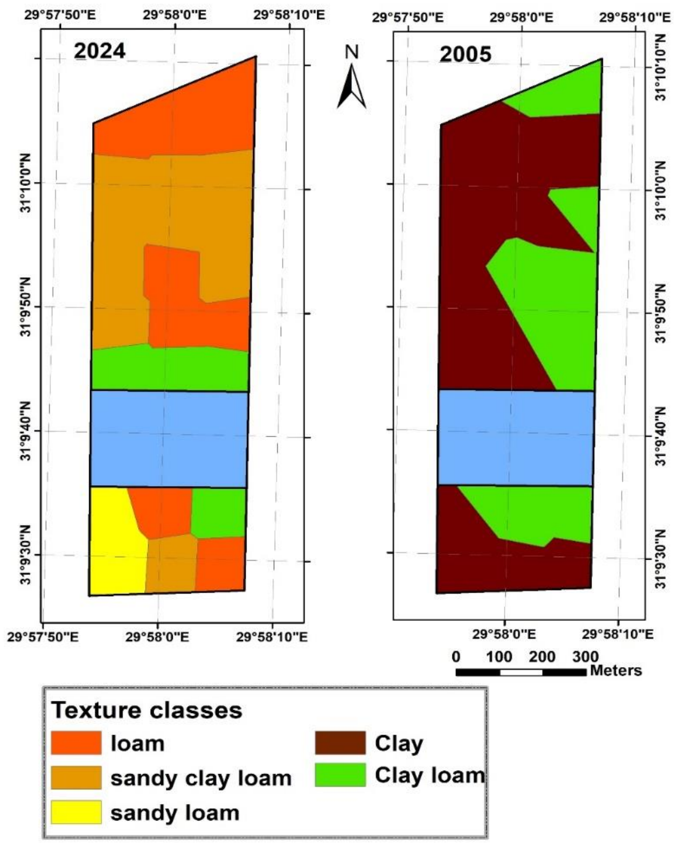

Map(6) Distribution of Texture and changes detected between 2005 and 2024 in the study area

Soil texture distributions exhibited substantial transformation between survey periods (2005 vs. 2024). Contemporary data show Sandy Clay Loam as the dominant textural class (~40% areal coverage), with Loam comprising >36.5% of the study area. This represents a fundamental departure from the 2005 baseline where Clay textures dominated (>63.5% coverage). This textural transition from cohesive clays to coarser Loam/Sandy Clay Loam fractions suggests substantial topsoil restructuring, potentially linked to groundwater-induced particle segregation or mechanized puddling effects (Zhang et al., 2021).

Table(7) Areas and percentages of O.M classes

	2024			2005		
O.M%	**Hectare**	**Feddan**	**%**	**Hectare**	**Feddan**	**%**
0.5-1.5				4.14	9.89	11.15
1.5-1.7	5.73	13.70	15.44	26.49	63.30	71.33
1.7-2	20.16	48.19	54.30	6.50	15.55	17.52
2-3	11.24	26.85	30.26			
Total	**37.13**	**88.74**	**100**	**37.13**	**88.74**	**100**

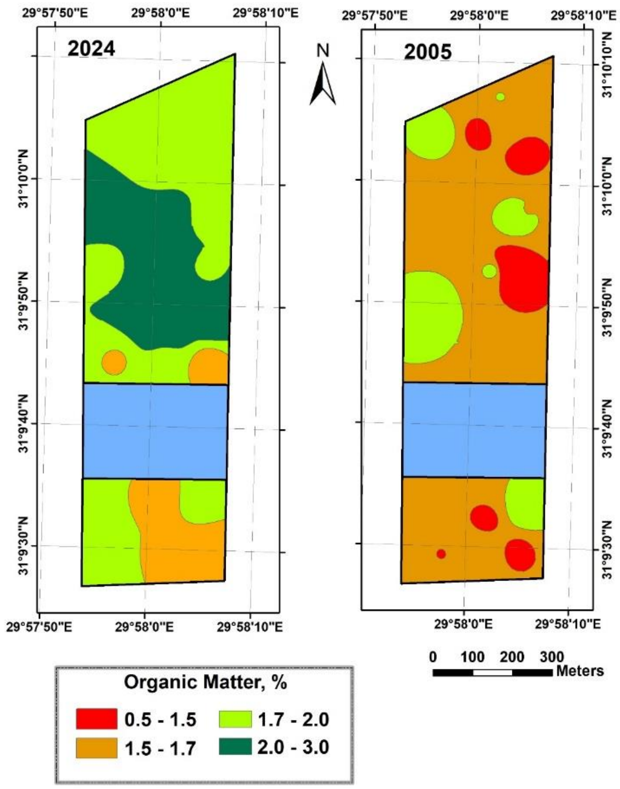

Map (7) Distribution of O.M. and changes detected between 2005 and 2024 in the study area

Tabular and spatial data reveal progressive enrichment of soil organic matter (SOM) within the study area. The 2024 survey demonstrates that the 1.7–2% SOM range now dominates, occupying 54.3% of the area, followed by the 2–3% range at >30% coverage. Collectively, >84% of soils exceed 1.7% SOM – a fundamental redistribution from the 2005 baseline, where the predominant SOM range (1.5–1.7%) covered 71.3% of the study area. This SOM elevation likely reflects: (a) legacy rice-crop residues increasing carbon inputs (Bana et al., 2023), (b) reduced mineralization rates under shallow water tables (Kögel-Knabner et al., 2008), (c) clay-SOM complexation stabilizing accumulated carbon (FAO, 2021).

Table(8) Areas and percentages of N classes

2024				2005			
Nitrogen, mg/kg soil	**Hectares**	**Feddan**	**%**	**Nitrogen mg/kg soil**	**Hectares**	**Feddan**	**%**
20-30	18.30	43.75	49.29	65-70	6.43	15.38	17.33
30-40	12.68	30.29	34.14	70-75	16.52	39.48	44.49
40-50	6.153	14.71	16.57	75-80	11.09	26.52	29.88
				80-85	3.08	7.36	8.30
Total	**37.13**	**88.75**	**100**		**37.13**	**88.74**	**100**

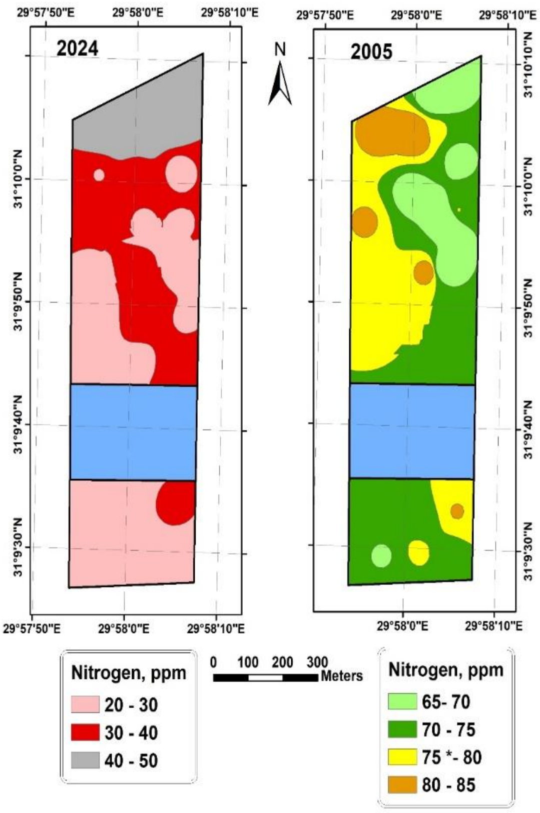

Map (8) Distribution of N and changes detected between 2005 and 2024 in the study area

Tabulated and spatial data demonstrate a severe depletion of soil available nitrogen (N) between sampling intervals (2005 vs. 2024). The current survey reveals only 16.5% of the study area contains the highest available N range (40–50 mg/kg soil), while the most extensive fraction (49.3%) falls within the critically low 20–30 mg/kg range. This contrasts fundamentally with the 2005 baseline, where 44.5% of soils contained abundant available N (70–75 mg/kg), and even the lowest category (65–70 mg/kg) still covered 17.3% of the area – indicating a region-wide N mining phenomenon. This N depletion likely reflects: (a) mineralization-suppressing anaerobic conditions under elevated water tables (Kirk et al., 2022), (b) legacy rice cultivation exhausting N reserves without adequate fertilization (Pampolino et al., 2023), (c) ammonia volatilization exacerbated by high pH from $CaCO_3$ accumulation (Sapkota, 2024), (d) arid to semi-arid climate further exacerbates N depletion (Tubeileh and Thomas, 2023).

Table(9) Areas and percentages of P classes

	2024			2005		
Phosphorous mg/kg soil	**Hectares**	**Feddan**	**%**	**Hectares**	**Feddan**	**%**
5-10				20.05	47.92	54.00
10-16	9.42	22.51	25.37	3.50	8.37	9.43
16-18	12.70	30.36	34.21	4.53	10.84	12.21
18-20	15.01	35.87	40.42	9.04	21.61	24.36
total	**37.13**	**88.73**	**100**	**37.13**	**88.74**	**100**

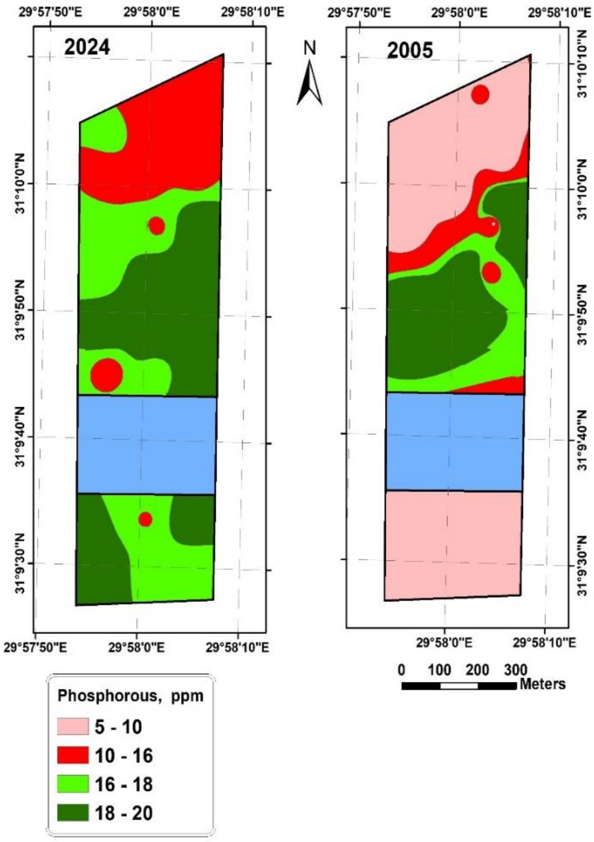

Map (9) Distribution of P and changes detected between 2005 and 2024 in the study area

The table and map depicting the soil phosphorus content for the years 2005 and 2024 illustrate a significant improvement in the phosphorus levels in 2024 as compared to 2005. Approximately 54% of the study area in 2005 had phosphorus levels below 10 mg/kg of soil, as highlighted in the table and map. However, by 2024, the entire study area had phosphorus levels above 10 mg/kg of soil. Even though the study area's soils tend to be calcareous, which means they have a high content of calcium carbonate, the increase in available phosphorus between 2005 and 2024 is a result of adaptive soil-plant processes and phosphorus accumulation over time (Li et al., 2024). Over time, phosphorus fertilizers may have exceeded the soils fixation thresholds and began to fully saturate calcium binding sites, which in turn increased the P fraction that is easy to extract. Moreover, the addition of organic matter combined with soil conservation measures has increased microbial activity and organic acid secretion, which helps to solubilize phosphorus, even in alkaline soils. Microbially mediated acidification and processes in the root zone aid in the calcium-phosphate phosphorus solubilizing and mobilizing (Wang et al., 2023). Collectively, these mechanisms offset the immobilizing effect of calcium carbonate, enabling a sustained rise in plant-available phosphorus despite calcareous conditions.

Table(10) Areas and percentages of K classes

2024				2005			
Potassium mg/kg soil	Hectares	Feddan	%	Potassium mg/kg soil	Hectares	Feddan	%
60-80	12.47	29.81	33.59	15-25	5.81	13.87	15.64
80-100	15.71	37.54	42.30	25-35	21.95	52.45	59.11
100-120	8.95	21.39	24.11	35-45	9.38	22.41	25.25
Total	37.13	88.74	100		37.13	88.74	100

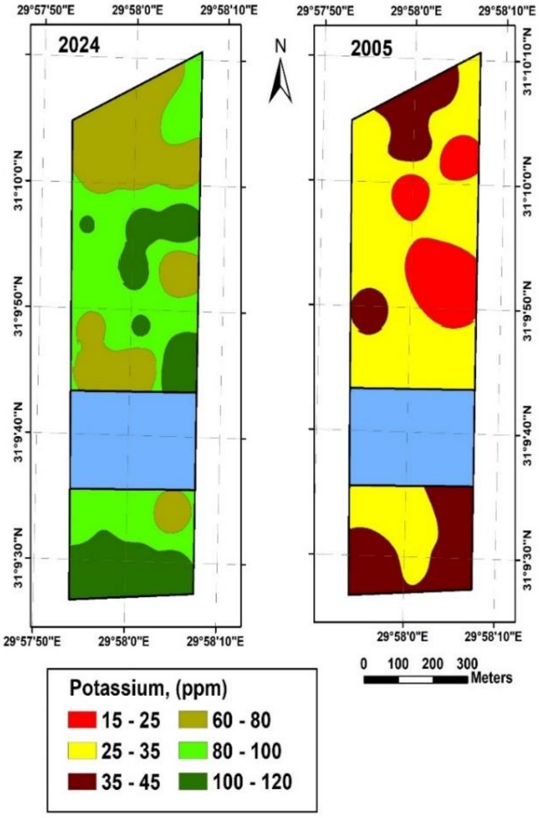

Map (10) Distribution of K and changes detected between 2005 and 2024 in the study area

A substantial augmentation in the bioavailable potassium content in soils was documented over the period from 2005 to 2024. In 2005, the maximum measured concentration of soil-available potassium was 45 mg/kg, with approximately 75% of the surveyed land exhibiting potassium levels greater than 35 mg/kg. Conversely, data from 2024 indicate a pronounced upward shift, with the lowest detected concentration ranging between 60 and 80 mg/kg, encompassing about 35.5% of the studied area, while 42.3% of the land showed elevated availability levels between 80 and 100 mg/kg of soil-available potassium.

The changes in soil potassium in paddy fields extracted from dried lacustrine during the last 20 years—the lacustrine having a calcium carbonate rich soil and found in arid to semi-arid areas—is due to different reasons:(1) The lacustrine sediments have some degree of potassium as well as fine sediment containing clay that can retain potassium and prevents leaching even rainfall is low, resulting in limited leaching losses (Sardans and Peñuelas, 2021). (2)The practice of growing rice continuously brings additional organic matter as well as regular potassium application resulting in a sustained soil potassium increase (Keller et al., 2020). (3) The high content of calcium carbonate in the soil also enhances the availability of potassium by preventing its fixation in exchange sites (Guo et al., 2019). (4) The potassium leaching that can occur in arid and semi-arid areas is considerably lower resulting in the potassium concentrating in the upper horizons (Tubeileh and Thomas, 2023).

Conclusion:

In conclusion, this study confirms that the observed changes in soil properties in the study area between 2005 and 2024 reflect the influence of various environmental factors and possibly human activities. The comparison indicates some improvements, as well as some changes that deserve attention. The results of this comparison also contribute to improving land management strategies and guiding agricultural policies in a scientifically sound manner.

Recommendations:

1. Continuous monitoring: It is essential to maintain regular and accurate measurements of soil properties to ensure early detection of any future changes.
2. Adopting sustainable agricultural practices: It is recommended to implement agricultural methods that preserve soil quality and reduce salinity.
3. Future studies: It would be useful to conduct similar studies over future periods to track further changes more accurately.
4. Adopting advanced technologies for more accurate soil assessment.
5. Aligning agricultural policies with research findings to maximize land use efficiency.

REFERENCES

Agatova, A. R., Nepop, R. K., Moska, P., Nikitenko, B. L., Bronnikova, M. A., Zhdanova, A. N., Zazovskaya, E. P., Karpukhina, N. V., Kuzmina, O. B., Nepop, A. R., Ovchinnikov,. I. Yu., Petrozhitskiy, A. V., & Uspenskaya, O. N. (2023, June). Recent data of multidisciplinary studies of the major Pleistocene climatic events: Glaciations, formation of ice-dammed lakes, and their catastrophic drainage in Altai (Mountains of Southern Siberia). In *Doklady Earth Sciences* (Vol. 510, No. 2, pp. 459-464). Moscow: Pleiades Publishing.

Almutairi, A., & Warner, T. A. (2010). Change detection accuracy and image properties: a study using simulated data. *Remote Sensing*, *2*(6), 1508-1529.

Bana, R. S., Bamboriya, S. D., Kumar, V., Godara, S., Gaydon, D. S., Laing, A. M., Dhakar, R., Shivay, Y. S., Meena, V. S., & Singh, D. (2023). Identifying optimum residue levels for stable crop and water productivity and carbon sequestration under a conservation agriculture based rice-wheat system. *Soil and Tillage Research*, *232*, 105745.

Banian, S. (2021). *Content-Aware AI-Driven Design Assistance Frameworks for Graphic Design Layouts* (Doctoral dissertation, Northeastern University).

Bouman, B. A., Humphreys, E., Tuong, T. P., & Barker, R. (2007). Rice and water. *Advances in agronomy*, *92*, 187-237.

Bungau, S., Behl, T., Aleya, L., Bourgeade, P., Aloui-Sossé, B., Purza, A. L., Abid, A., & Samuel, A. D. (2021). Expatiating the impact of anthropogenic aspects and climatic factors on long-term soil monitoring and management. *Environmental Science and Pollution Research*, *28*(24), 30528-30550.

Cohen, A. B., Klepac-Ceraj, V., Bidas, K., Weber, F., Garber, A. I., Christensen, L. N., Cram, J. A., McCormick, M. L., & Taylor, G. T. (2023). Deep photoautotrophic prokaryotes contribute substantially to carbon dynamics in oxygen-deficient waters in a permanently redox-stratified freshwater lake. *Limnology and Oceanography*, *68*(1), 232-247.

Dingman, S. L. (2015). ***Physical hydrology*****. Waveland press.**

Du, P., Liu, S., Xia, J., & Zhao, Y. (2013). Information fusion techniques for change detection from multi-temporal remote sensing images. *Information Fusion*, *14*(1), 19-27.

Duniway, M. C., Herrick, J. E., & Monger, H. C. (2010). Spatial and temporal variability of plant-available water in calcium carbonate-cemented soils and consequences for arid ecosystem resilience. *Oecologia*, *163*(1), 215-226.

ESRI (2021). ArcGIS 10.8 user's manual. Redlands, CA, USA.

FAO (2021). Saline Agriculture. *Future of Sustainable Agriculture in Saline Environments*, 1.

FAO. (2021). Carbon accumulation in arable soils: Mechanisms and the effect of cultivation practices and organic fertilizers. *Agronomy*, *11*(6), 1079.

Fisichella, M., & Garolla, F. (2021). Can deep learning improve technical analysis of forex data to predict future price movements?. *Ieee Access*, *9*, 153083-153101.

Guo, J., Jia, Y., Chen, H., Zhang, L., Yang, J., Zhang, J., Hu, X., Ye, X., Li, Y., & Zhou, Y. (2019). Growth, photosynthesis, and nutrient uptake in wheat are affected by differences in nitrogen levels and forms and potassium supply. *Scientific reports*, *9*(1), 1248.

Hemati, M., Hasanlou, M., Mahdianpari, M., & Mohammadimanesh, F. (2021). A systematic review of landsat data for change detection applications: 50 years of monitoring the earth. *Remote sensing*, *13*(15), 2869.

IFAD, (1991). Egypt West Nubaria Intensification Project, IFAD/WB/GOE

Jackson, M. L. (1973). *Soil chemical analysis-advanced course: A manual of methods useful for instruction and research in soil chemistry, physical chemistry of soils, soil fertility, and soil genesis*. author.

Jiang, W., Sun, Y., Lei, L., Kuang, G., & Ji, K. (2024). Change detection of multisource remote sensing images: a review. *International Journal of Digital Earth*, *17*(1), 2398051**.**

Jim, C. Y. (2023). Rootability confinement and soil-husbandry solutions for urban trees in sealed and insular sites. *Plant and Soil*, *483*(1), 153-180.

Keller, P. S., Catalán, N., von Schiller, D., Grossart, H. P., Koschorreck, M., Obrador, B., Frassl, M. A., Karakaya, N., Barros, N., Howitt, J. A., Mendoza-Lera, C., Pastor, A., Flaim, G., Aben, R., Riis, T., Arce, M. I., Onandia, G., Paranaíba, J. R., Linkhorst, A., del Campo, R., Amado, A. M., Cauvy-Fraunié, S., Brothers, S., Condon, J., & Marcé, R. (2020). Global CO2 emissions from dry inland waters share common drivers across ecosystems. *Nature communications*, *11*(1), 2126**.**

Kirk, G. J., Manwaring, H. R., Ueda, Y., Semwal, V. K., & Wissuwa, M. (2022). Below-ground plant–soil interactions affecting adaptations of rice to iron toxicity. *Plant, Cell & Environment*, *45*(3), 705-718.

Kirk, J. L., Beaudette, L. A., Hart, M., Moutoglis, P., Klironomos, J. N., Lee, H., & Trevors, J. T. (2004). Methods of studying soil microbial diversity. *Journal of microbiological methods*, *58*(2), 169-188.

Kögel-Knabner, I., Guggenberger, G., Kleber, M., Kandeler, E., Kalbitz, K., Scheu, S., Eusterhues, K., & Leinweber, P. (2008). Organo-mineral associations in temperate soils: Integrating biology, mineralogy, and organic matter chemistry. *Journal of Plant Nutrition and Soil Science*, *171*(1), 61-82.

Kuehne, L. M., Habtour, E., Echenagucia, T. M., & Orfield, S. J. (2025). Technology-forcing to reduce environmental noise pollution: a prospectus. Journal of Exposure Science & Environmental Epidemiology, 35(1), 6-15.

Li, J., Xie, H., Li, J., Yang, G., Xie, Y., Wang, J., Zhou, C., & Zou, S. (2023). Influences of anthropogenic acids on carbonate weathering and CO2 sink in an agricultural karst wetland (South China). *Ecological Indicators*, *150*, 110192.

Li, Y., Liu, M., Wang, H., Li, C., Zhang, Y., Dong, Z., Fu, C., Ye, Y., Wang, F., Chen, X., & Wang, Z. (2024). Effects of different phosphorus fertilizers on cadmium absorption and accumulation in rice under low-phosphorus and rich-cadmium soil. *Environmental Science and Pollution Research*, *31*(8), 11898-11911.

Liu, C., Chen, K., Zhang, H., Qi, Z., Zou, Z., & Shi, Z. (2024). Change-agent: Towards interactive comprehensive remote sensing change interpretation and analysis. IEEE Transactions on Geoscience and Remote Sensing.

Ma, Y., Ke, P., Aghababaei, H., Chang, L., & Wei, J. (2024). Despeckling sar images with log-yeo-johnson transformation and conditional diffusion models. IEEE Transactions on Geoscience and Remote Sensing.

Mas, J. F. (1999). Monitoring land-cover changes: a comparison of change detection techniques. International journal of remote sensing, 20(1), 139-152.

MH Yossif, T. (2017). Change detection of land cover and salt affected soils at Siwa Oasis, Egypt. *Alexandria Science Exchange Journal*, *38*(July-September), 446-462.

Minhas, P. S., & Qadir, M. (2024). Agroclimate-centric irrigation water quality guidelines. *Irrigation and Drainage*, *73*(4), 1592-1605.

Montero-Rosado, C., Ojeda-Trejo, E., Espinosa-Hernández, V., Fernández-Reynoso, D., Caballero Deloya, M., & Benedicto Valdés, G. S. (2023). Historical Political Ecology in the Former Lake Texcoco: Hydrological Regulation. *Land*, *12*(5), 1113.

Onishi, M., & Ise, T. (2021). Explainable identification and mapping of trees using UAV RGB image and deep learning. *Scientific reports*, *11*(1), 903.

Page, A., R. H. Miller and R. Keeny (1982). Methods of soil analysis. Part 2.

Pampolino, M. F., Laureles, E. V., Gines, H. C., & Buresh, R. J. (2008). Soil carbon and nitrogen changes in long-term continuous lowland rice cropping. *Soil Science Society of America Journal*, *72*(3), 798-807.

Parker, L., & Prabawa-Sear, K. (2020). *Environmental education in Indonesia: creating responsible citizens in the global south?* (p. 280). Taylor & Francis.

Perego, R., Furlanetto, G., Rapi, M., & Ravazzi, C. (2025). Plant-human interactions: from pristine forest to Bronze Age farming—vegetation history and depositional processes off-shore the lake dwelling of Lavagnone, N-Italy. *Vegetation History and Archaeobotany*, 1-29.

Prazina, I., Bećirović, Š., Cogo, E., & Okanović, V. (2023). Methods for Automatic Web Page Layout Testing and Analysis: A Review. *IEEE Access*, *11*, 13948-13964.

Richards, L. A. (1954). Diagnosis and Improvement of saline and alkaline soil. U.S. Regional Salinity Lab. Riverside, Calif. USA.

Ritzema, H. P., & Braun, H. M. H. (1994). Environmental aspects of drainage.

Rudaya, N., Nazarova, L., Frolova, L., Palagushkina, O., Soenov, V., Cao, X., Syrykh, L., Grekov, I., Otgonbayar, D., Bayarkhuu, B., & Bayarkhuu, B. (2021). The link between climate change and biodiversity of lacustrine inhabitants and terrestrial plant communities of the Uvs Nuur Basin (Mongolia) during the last three millennia. *The Holocene*, *31*(9), 1443-1458.

Said, R. (1962). The Geology of Egypt, El Sevier Publ. *Comp. Amsterdam, New York*.

Sapkota, S. (2024). *Optimization of Ammonia Nitrogen Removal and Recovery from Undigested Screened Dairy Manure Using Vacuum Thermal Stripping and Acid Absorption Process: A Modeling Approach Using Response Surface Methodology* (Master's thesis, University of Idaho).

Sardans, J., & Peñuelas, J. (2021). Potassium control of plant functions: Ecological and agricultural implications. *Plants*, *10*(2), 419.

Shi, W., Zhang, M., Zhang, R., Chen, S., & Zhan, Z. (2020). Change detection based on artificial intelligence: State-of-the-art and challenges. *Remote Sensing*, *12*(10), 1688.

Stringer, C. A., & Prendergast, A. L. (2023). Freshwater mollusc sclerochronology: Trends, challenges, and future directions. *Earth-Science Reviews*, *247*, 104621.

Stuart-Street, A, Short, N., Galloway, P. & Schoknecht, N. (2020) A simple guide for describing soils, Department of Primary Industries and Regional Development, Perth.

Sun, W., Jiang, Q., Liu, E., Chang, J., & Zhang, E. (2018). Climate change dominates recent sedimentation and organic carbon burial in Lake Chenghai, southwest China. *Journal of Limnology*, *77*(3).

Tubeileh, A. M., & Thomas, R. J. (2023). The Management of Soil Systems in Arid and Semi-Arid Climates. In *Biological Approaches to Regenerative Soil Systems* (pp. 55-66). CRC Press.

Vetráková, H. (2023). *Navigating the complexities of forest management policies in the Czech Republic: the role of LULUCF regulation in mitigating climate change* (Master's thesis, Norwegian University of Life Sciences, Ås).

Walter, J., Chesnaux, R., Boumaiza, L., Brindha, K., & Regenspurg, S. (2023). Conceptual model for the chemical evolution of groundwater in a region of the Canadian Precambrian shield covered by soft Quaternary deposit of glacial and marine origin. *Applied Geochemistry*, *150*, 105574.

Wang, L., Wang, J., Yuan, J., Tang, Z., Wang, J., & Zhang, Y. (2023). Long-term organic fertilization strengthens the soil phosphorus cycle and phosphorus availability by regulating the pqqC-and phoD-harboring bacterial communities. *Microbial Ecology*, *86*(4), 2716-2732.

Wang, L., Zeng, X., & Yu, H. (2022). Association between lake sediment nutrients and climate change, human activities: a time-series analysis. *Environmental Management*, *70*(1), 117-133.

Wen, D., Huang, X., Bovolo, F., Li, J., Ke, X., Zhang, A., & Benediktsson, J. A. (2021). Change detection from very-high-spatial-resolution optical remote sensing images: Methods, applications, and future directions. *IEEE Geoscience and Remote Sensing Magazine*, *9*(4), 68-101.

Wu, F., You, Q., Zhang, Z., & Zhang, L. (2021). Changes and uncertainties of surface mean temperature over China under global warming of 1.5 and 2° C. *International Journal of Climatology*, *41*, E410-E427.

Yang, N., Zhang, C., Wang, L., Li, Y., Zhang, W., Niu, L., Zhang, H., & Wang, L. (2021). Nitrogen cycling processes and the role of multi-trophic microbiota in dam-induced river-reservoir systems. *Water Research*, *206*, 117730.

Yehia, H. A., ElGhonamey, Y. K., & Elshemy, A. S. A. (2014). Application of Geographic Information System Using ALES-ARID Module for Land Evaluation Assessment of Abis area, WestDelta, Egypt. Soil Salinity and Alkalinity Research Lab. Soil, Water and Environment Research institute (SWERI), Giza. J. Agric. Res, 39(2), 831-851.

, *16*(22), 4169.

Zamanian, K., Zhou, J., & Kuzyakov, Y. (2021). Soil carbonates: The unaccounted, irrecoverable carbon source. *Geoderma*, *384*, 114817**.**

Zhang, S., Huang, G., Zhang, Y., Lv, X., Wan, K., Liang, J., Feng, Y., Dao, J., Wu, S., Zhang, L., Yang, X., Lian, X., Huang, L., Shao, L., Zhang, J., Qin, S., Tao, D., Crews, T. E., Sacks, E. J., Lyu, J., Wade L. J., & Hu, F. (2023). Sustained productivity and agronomic potential of perennial rice. *Nature Sustainability*, *6*(1), 28-38.

Zhang, Y., Liu, Q., Zhang, W. D., Wang, X. H., Mao, R., Tigabu, M., & Ma, X. Q. (2021). Linkage of aggregate formation, aggregate-associated C distribution, and microorganisms in two different-textured ultisols: A short-term incubation experiment. *Geoderma*, 394, 114979.

Zheng, Z., Wang, J., Ni, J., Cui, Y., & Zhu, Q. (2024). Lacustrine Wetlands Landscape Simulation and Multi-Scenario Prediction Based on the Patch-Generating Land-Use Simulation Model: A case study on shengjin lake reserve, china. *Remote Sensing*

الملخص العربي

تتبع تغيرات التربة البحيرية في منطقة ابيس ، محافظة الاسكندرية ، مصر

هدى عبد الفتاح محمود[1] ايهاب محرم محمد مرسي[2]

علا سعد علواني[1] اسلام ابراهيم ابو السعود[1]

1كلية الزارعة سابا باشا – جامعة الاسكندرية – مصر

معهد بحوث الاراضي والمياه والبيئة – مركز البحوث الزارعية – الجيزة – مصر2

تُعَدُّ التربة الناتجة من الترسيبات البحيرية مكوّناً أساسياً ودائماً من مكوّنات النظم البيئية الطبيعية، وترتبط ارتباطاً وثيقاً بكلٍ من الاستقرار البيئي والأنشطة البشرية. ويُعَدُّ رصد وتحليل التغيرات التي تطرأ على هذه الانواع من الاراضي عبر الزمن أمراً ضرورياً لتقييم صحة النظم البيئية، وتقدير مخاطر تدهور الأراضي، وتوجيه استراتيجيات الحفاظ عليها. تهدف هذه الدراسة إلى رصد وتوثيق التغيرات في الخواص الفيزيائية والكيميائية للتربة الناتجة من الترسيبات البحيرية، مع التركيز على المقارنة بين حالتها في عامي 2005 و2024. وقد أُجريت الدراسة على مساحة 109.6 فدان (45.86 هكتار) في القرية 10 بمنطقة أبيس، ضمن نطاق محافظة الإسكندرية، مصر. استندت البيانات إلى صور الأقمار الصناعية لاندسات لعام 2024 بالإضافة إلى القياسات الحقلية لعينات التربة. تم جمع 48 عينة تربة بواقع 24 عينة سطحية و24 عينة تحت سطحية، لتغطية مساحة قدرها 88.7 فدان. تضمنت التحاليل مجموعة شاملة من المؤشرات الفيزيائية والكيميائية لكلٍ من التربة والمياه، بما في ذلك: قوام التربة، التوصيل الكهربائي (EC, dS/m)، تفاعل التربة (pH)، الكاتيونات والأنيونات الذائبة، نسبة امتصاص الصوديوم(SAR) ، محتوى كربونات الكالسيوم($CaCO_3$) ، المادة العضوية، إضافة إلى تركيزات النيتروجين والفوسفور والبوتاسيوم المتاح. ولإنتاج خرائط رقمية لحالة التربة في عام 2024، تم إدخال البيانات المكانية (النقاط، والخطوط، والمساحات) وربطها بالبيانات الوصفية (رقمية ونصية) باستخدام نظم المعلومات الجغرافية(GIS) . أظهرت النتائج زيادة ملحوظة في محتوى كربونات الكالسيوم في عام 2024 مقارنة بعام 2005، إلى جانب ارتفاع في ملوحة التربة، وزيادة محتوى المادة العضوية، وارتفاع مستويات الفوسفور والبوتاسيوم المتاحين. وفي المقابل، لوحظ انخفاض في عمق التربة ومحتوى النيتروجين المتاح. كما سُجِّل تغير واضح في قوام التربة؛ إذ كانت تصنَّف في عام 2005 ضمن فئات Clay, Clay loam، بينما تحولت في عام 2024 إلى قوامات Loam, Sandy clay loam, Sandy loam. تُسهم هذه النتائج في توفير أساس علمي راسخ لتحسين استراتيجيات إدارة الأراضي وتوجيه السياسات الزراعية، لاسيما في البيئات البحيرية الواقعة ضمن المناطق الجافة وشبه الجافة حيث يُعَد الاستخدام المستدام للتربة أمراً بالغ الأهمية.